

Structural and electrical conductivity studies on rutile solid solutions $[\text{Fe}_x\text{Ti}_{1-2x}\text{M}_x\text{O}_2$ ($\text{M} = \text{Nb}, \text{Ta}$)]

P. ESCRIBANO, F. FABREGAT*, G. GARCIA-BELMONTE*, E. CORDONCILLO, J. BISQUERT*, M. A. TENA

*Inorganic Chemistry Area, Inorganic and Organic Chemistry Department and *Applied Physics Area, Experimental Science Department, Universitat Jaume I, E-12080 Castelló, Spain*

In this study, $\text{Fe}_x\text{Ti}_{1-2x}\text{M}_x\text{O}_2$ ($\text{M} = \text{Nb}, \text{Ta}$; $0 \leq x \leq 0.5$) solid solutions have been synthesized from both ceramic and gel methods, and electrical and structural characterization has been carried out. The solid solutions show rutile structure except for the case of FeNbO_4 , which forms an orthorhombic structure. The electrical behaviour of the system studied corresponds to extrinsic p-type semiconduction and it is related to the presence of Fe(II) ions. Conductivity is enhanced by local distortions of the M–O lengths associated with ordering oxidation states such as those in Fe_3O_4 . The distortions are more frequent when the asymmetry is greater ($\text{M} = \text{Nb}$). No electrical changes have been detected when the synthesis method is different. © 1998 Kluwer Academic Publishers

1. Introduction

TiO_2 in the rutile modification forms solid solutions with other transition metal oxides with rutile-related structures. In most cases, undistorted rutile structures are formed and the properties of the transition metal oxides are modified by the presence of TiO_2 [1].

A few articles have been dedicated to electrical characterization studies of this type of solid solutions. Members of the series $\text{Fe}_{x/3}\text{Nb}_{2x/3}\text{Ti}_{1-x}\text{O}_2$ ($x = 0.1, 0.2, 0.3$) were synthesized and their electrical and magnetic properties studied by Khazai *et al.* [2]. Resistivity measurements for these compositions gave values of the order of $10^6 \Omega \text{ cm}$ at 300 K. The high resistivity was attributed to a random distribution of the ions in the rutile structure.

As described in previous papers on synthesis of rutile solid solutions [3, 4], $\text{Fe}_x\text{Ti}_{1-2x}\text{M}_x\text{O}_2$ ($\text{M} = \text{Nb}, 0 \leq x \leq 0.4$ and $\text{M} = \text{Ta}, 0 \leq x \leq 0.5$) rutile solid solutions were obtained. When $\text{M} = \text{Ta}$, two phases with rutile structure (TiO_2 and TaFeO_4) were found from ceramic samples and only one phase with rutile structure (rutile solid solution) was obtained from gel methods at 1000°C . The absence of the TaFeO_4 compound formation indicated a higher homogeneity in gel samples. When $\text{M} = \text{Nb}$, the rutile phase was not detected for $x = 0.5$ in both ceramic and gel samples due to formation of FeNbO_4 with orthorhombic structure.

Many metal oxides containing a transition metal element are mixed valence compounds, in which the valence can not be assigned to a unique integral oxidation state. This category includes not only the non-stoichiometric and doped compounds, but also many

stoichiometric ones such as Fe_3O_4 [5]. In this sense, FeNbO_4 , a high conductive extrinsic semiconductor [6], could be a mixed valence oxide with Fe(II) and Fe(III). The presence of Fe(II) may be due to a charge transfer from the oxide ions to the Fe(III) ions [7].

The aim of this study is the electrical characterization of $\text{Fe}_x\text{Ti}_{1-2x}\text{M}_x\text{O}_2$ ($\text{M} = \text{Nb}, \text{Ta}$) solid solutions, in order to determine the influence of composition (Fe-M/Ti ratio), M(V) cation, crystalline structure, synthesis methods and sintering of powders on the electrical properties.

2. Experimental

Samples of $\text{Fe}_x\text{Ti}_{1-2x}\text{M}_x\text{O}_2$ ($\text{M} = \text{Nb}, \text{Ta}$; $0 \leq x \leq 0.5$) were prepared by three methods: ceramic (CE), colloidal gel (CG) and polymeric gel (PG) [4]. In the ceramic method, raw materials, TiO_2 anatase (Probus), Nb_2O_5 (Merck) or Ta_2O_5 (Merck) and Fe_2O_3 (Panreac), were mixed and homogenized in acetone in a ball mill. In the colloidal gel method, NbCl_5 (Merck) or TaCl_5 (Merck) was dispersed in water by vigorous stirring at 70°C and TiCl_4 (Merck) and $\text{FeCl}_3 \cdot 6\text{H}_2\text{O}$ (Panreac) were successively added. Then a solution of ammonium hydroxide was added dropwise until gelation ($\text{pH} = 5\text{--}6$) occurred. Finally, in the polymeric gel method, a solution of NbCl_5 (Merck) or Ta(V) ethoxide (Merck) in ethanol was refluxed with continuous stirring at 70°C and Fe(III) acetylacetonate and Ti(IV) isopropoxide were added successively and acidified with 3 M HNO_3 .

All the samples obtained were dried in air at room temperature (20°C) and were fired in refractory

crucibles at temperatures between 300 and 1000 °C for 12 h of soaking time. The resulting materials were ceramically conformed into disk pellets (1.0 cm diameter, 2–5 mm thick) and then sintered in air at (a) 1450 °C for 2 h and (b) 1400 °C for 10 h.

The disk pellet densities were measured and the pellets analysed by X-ray diffraction using CuK_α radiation and a Ni filter in order to study the crystalline phases in them. In some samples, a structure profile refinement was carried out by the Rietveld method [8] with the data obtained by means of a Siemens D5000 X-ray diffractometer with CuK_α radiation in the $(10\text{--}70)^\circ 2\theta$ Bragg angle interval.

Samples for electrical tests were electroded onto both surfaces with platinum high-conductivity paste. These contacts were fired at 800 °C for 2 h. For impedance complex plane analysis, a frequency analyser HP-4192A in the frequency range of 5–10⁷ Hz was employed. Samples were placed in a hot-sample holder regulated by a temperature controller and measurements were carried out between 20 and 300 °C. Measurements of the thermoelectric power sign show that we are dealing with p-type semi-conductors.

Data from impedance spectroscopy measurements were fitted to equivalent electrical circuits, which account for several conduction processes inside the samples. Details of the impedance data treatment can be found in [6], where a full characterization of FeNbO_4 was carried out.

With the aim of verifying the presence of Fe(II) in the samples, we have carried out Mössbauer spectroscopic measurements at room temperature. The employed radiation source was ⁵⁷Co and the velocity scale was calibrated using the hyperfine spectra of a natural α -iron foil, which also served as the isomer shift reference.

3. Results and discussion

3.1. Structural characterization

The diffractograms of all the samples conformed in disk pellets indicate that only a phase with rutile structure was detected, except when $M = \text{Nb}$ and $x = 0.5$, in which an orthorhombic phase was observed and attributed to the presence of FeNbO_4 with orthorhombic structure.

Figs 1 and 2 show the rutile unit cell parameters and the interatomic distances $M\text{--O} (\times 4)$ and $M\text{--O} (\times 2)$ obtained from the structure profile refinement for fired samples at 1300 °C for the rutile solid solutions. It can be observed that cell parameters and distances increase linearly as x increases. This is in agreement with Vegard's law, as we are replacing Ti by larger ions (Fe, Ta and Nb). When $M = \text{Ta}$, the a values are slightly smaller and the c values are similar than in the case of $M = \text{Nb}$. On the other hand, when $M = \text{Nb}$ the difference between the distances $M\text{--O} (\times 4)$ and $M\text{--O} (\times 2)$ is related to the distortion in the octahedral site of M in the rutile structure, while no significant difference is detected in the distances when $M = \text{Ta}$. Thus, in rutile solid solutions the symmetry of the octahedral is higher in the case of $M = \text{Ta}$.

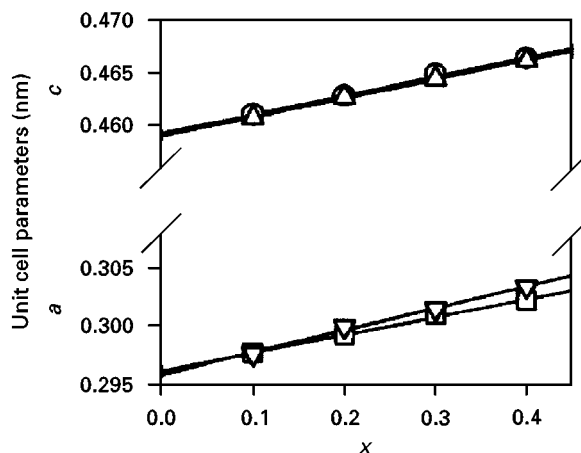


Figure 1 Unit cell parameters of rutile structure in $\text{Fe}_x\text{Ti}_{1-2x}\text{M}_x\text{O}_2$ ($M = \text{Nb}$ (\circ , \square), Ta (\triangle , ∇)) samples prepared by ceramic method and fired at 1300 °C.

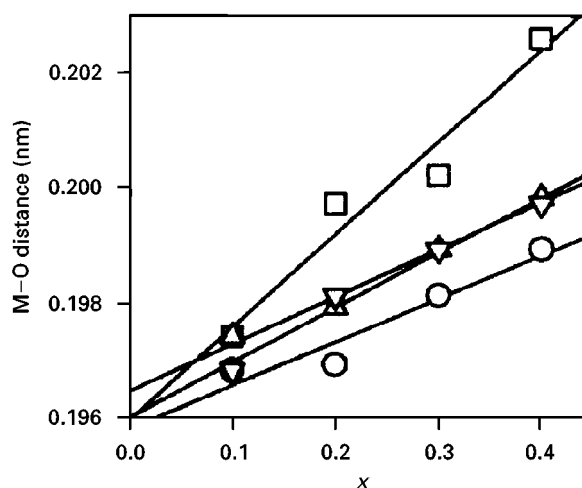


Figure 2 Interatomic $M\text{--O}$ distances in $\text{Fe}_x\text{Ti}_{1-2x}\text{M}_x\text{O}_2$ ($M = \text{Nb}$ (\circ) $\times 4$, (\square) $\times 2$), Ta (\triangle) $\times 4$, (∇) $\times 2$) rutile solid solutions prepared by ceramic method and fired at 1300 °C.

3.2. Electrical properties

Impedance spectra of most samples show only two arcs, the first associated with the bulk region and the second related to the material-electrode contacts [6]. In some instances ($M = \text{Ta}$, PG method at any x , CG method at $x = 0.5$ and $M = \text{Nb}$, CG method $x = 0.2$ and 0.4), a third arc appears, which is located between the other two. This third arc is attributed to the presence of grain boundaries, porosity, etc. [6], and indicates an unfulfilled sintering in those cases.

The bulk region electrical response consists of a pure $R\text{--}C$ parallel circuit in all samples, thus indicating a uniform structure in the intragrain material. Arrhenius plots (σ versus $1/T$) in the case of solid solutions containing Nb and Ta are shown in Fig. 3a and b, respectively. No significant changes as a function of the synthesis or sintering of powders procedure has been detected, therefore only ceramic samples have been represented in order to give clearer results.

The activation energies of the involved processes were calculated from the slope of the Arrhenius plots. This parameter results equal to 0.31 eV in the case

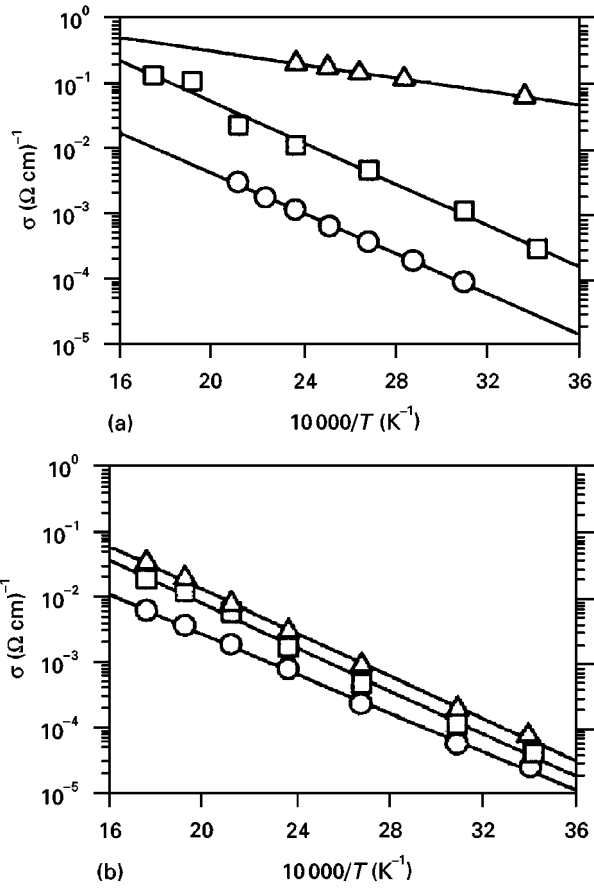


Figure 3 Arrhenius plots for ceramic method, 10h fired samples, (a) $M = \text{Nb}$ ($x = 0.2$ (O), 0.4 (□), 0.5 (△)) and (b) $M = \text{Ta}$ ($x = 0.2$ (O), 0.4 (□), 0.5 (△)).

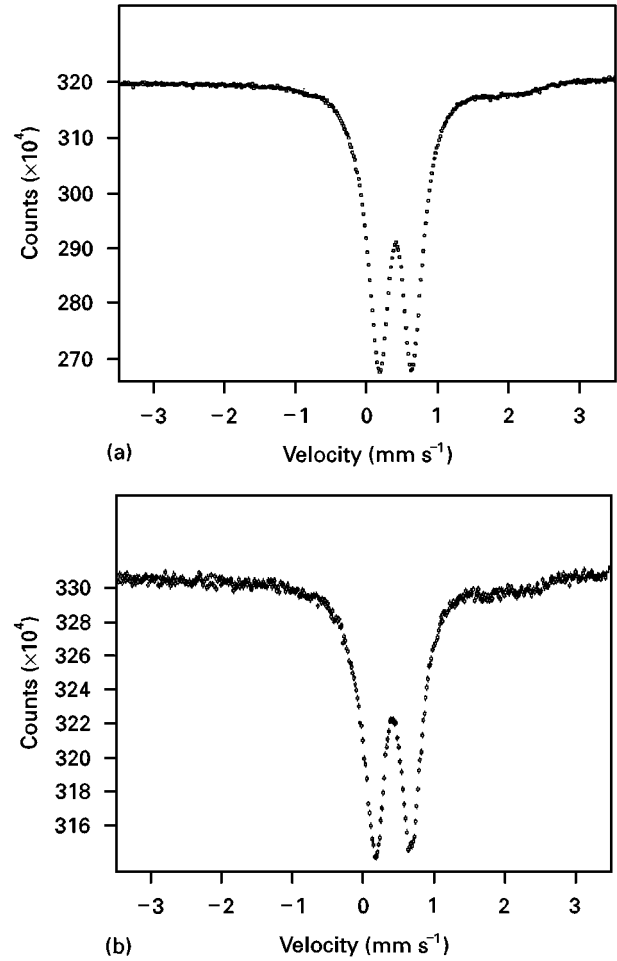


Figure 4 Mössbauer spectra, at room temperature, of (a) $M = \text{Nb}$ ($x = 0.4$) and (b) $M = \text{Ta}$ ($x = 0.4$).

TABLE I Mössbauer parameters estimated from the Mössbauer spectra, at room temperature, of the $\text{Fe}_x\text{Ti}_{1-2x}\text{M}_x\text{O}_2$ ($M = \text{Nb}, \text{Ta}$) ($x = 0.4$) solid solutions. Isomer shift with respect to the natural α -iron foil.

Sample ($x = 0.4$) M	Isomer shift (mm s^{-1})	Quadrupole splitting (mm s^{-1})	Curve width (mm s^{-1})	Relative intensity (%)
Nb				
1st doublet Fe(III)	0.418 (5)	0.450 (5)	0.385 (5)	92 (1)
2nd doublet Fe(II)	1.020 (2)	2.440 (2)	0.460 (2)	3 (1)
3rd sextet α - Fe_2O_3	0.383 (8)	-0.172 (8)	0.420 (2)	5 (1)
Ta				
1st doublet Fe(III)	0.425 (5)	0.508 (5)	0.385 (5)	92 (1)
2nd doublet Fe(II)	1.105 (2)	2.520 (2)	0.480 (2)	3 (1)
3rd sextet α - Fe_2O_3	0.384 (8)	-0.180 (8)	0.400 (2)	5 (1)

of $M = \text{Nb}$ and $x = 0.2, 0.4$, and it results 0.10 eV for $M = \text{Nb}$ and $x = 0.5$. This fact is attributed to the structural change from rutile to FeNbO_4 orthorhombic structure. On the other hand, the activation energy for the $M = \text{Ta}$ case, 0.32 eV , appears slightly higher than in the $M = \text{Nb}$ case and it is not dependent on the composition. These results correspond to a typical semiconducting behaviour, regarding both conductivity and activation energy values. The activation energy values of pure compounds (TiO_2 , Nb_2O_5 , Ta_2O_5 and Fe_2O_3) are too high to account for the measured energies [1].

The almost constant value of the activation energy, with the exception of the $M = \text{Nb}$ ($x = 0.5$) case, suggests that only one type of mechanism may be invoked to account for the electrical conduction process. We propose an electron exchange process (electron hopping) from oxide ions to Fe(III) [7] as a suitable explanation. With the aim of verifying the Fe(II) presence, we have carried out Mössbauer spectroscopic measurements at room temperature. Fig. 4 show an example of the obtained Mössbauer spectra, for the cases of $M = \text{Nb}$ ($x = 0.4$) and $M = \text{Ta}$ ($x = 0.4$), and Table I lists the corresponding Mössbauer

parameters. A small amount of Fe(II) is detected for all values of x . Therefore, data confirm the presence of the Fe(II) ion.

As can be observed in Fig. 3a, conductivity increases with x when $M = \text{Nb}$. This is in accordance with the change of the interatomic M–O distance (Fig. 2). In contrast, conductivity only suffers slight variations with x in the case of $M = \text{Ta}$, in good correlation with the symmetry of the cell. For the same value of x , conductivity is always higher when $M = \text{Nb}$. The difference of the conductivity values between the $M = \text{Nb}$ and $M = \text{Ta}$ cases is related to the deformation of the structure (Fig. 2). This deformation promotes local distortions of the M–O lengths and enhances electron transfer from oxide ions to Fe(III). Since structural symmetry is not distorted when $M = \text{Ta}$, the conductivity remains approximately constant. In conclusion, conductivity should be related simultaneously to both Fe(II) presence and cell distortion conditions.

4. Conclusions

From the experimental results discussed above, we conclude the following points about the $\text{Fe}_x\text{Ti}_{1-2x}\text{M}_x\text{O}_2$ ($M = \text{Nb}, \text{Ta}$) solid solutions:

(1) No dependence of the bulk conductivity or activation energy on the synthesis methods or sintering of powders procedure has been detected.

(2) The electrical behaviour of these rutile solid solutions corresponds to extrinsic p-semiconductors.

(3) In the solid solutions, the conductivity and activation energy should be related to the presence of Fe(II) ions. We have proposed an electron exchange process as a suitable explanation. Note that the activation energy values are almost constant, except for the case of $M = \text{Nb}$ ($x = 0.5$).

(4) The symmetry of the octahedral site of M in the rutile structure is higher when $M = \text{Ta}$ than when

$M = \text{Nb}$ and, therefore, the concentration of local distortions in the M–O bond lengths is smaller. This accounts for the different trends found in the electrical conductivity, namely, almost constancy when $M = \text{Ta}$ and large variations when $M = \text{Nb}$.

(5) When $x = 0.5$ and $M = \text{Nb}$, the electrical properties depart markedly from those of the rest of the solid solutions. This is accounted for by the change to orthorhombic structure in the case mentioned.

Acknowledgements

The authors are greatly indebted to Professor V. Kozhukharov, University of Chemical Technology and Metallurgy, Sofia, Bulgaria for the Mössbauer spectra. This work was supported by the Fundació Caixa-Castelló.

References

1. N. RAO and G. V. SUBBA RAO, COM-74-50715, National Standard Reference Data System (1975).
2. KHAZAI, R. KERSHAW, K. DWIGHT and A. WOLD, *Mater. Res. Bull.* **16** (1981) 655.
3. A. TENA, P. ESCRIBANO, G. MONRÓS, J. CARDA and J. ALARCÓN, *Mater. Res. Bull.* **27** (1992) 1301.
4. A. TENA, G. MONRÓS, J. CARDA, V. CANTAVELLA and P. ESCRIBANO, *J. Sol-Gel Sci. Technol.* **2** (1994) 381.
5. P. A. COX, "Transition Metal Oxides. An introduction to their electronic structure and properties" (Oxford Science Publications, Oxford) p. 32 and 242.
6. A. TENA, G. GARCIA-BELMONTE, J. BISQUERT, P. ESCRIBANO, M. T. COLOMER and J. R. JURADO, *J. Mater. Sci.* **31** (1996) 2043.
7. B. N. FIGGIS, "Introduction to Ligand Fields" (Interscience Publishers, 1967) pp. 245–247.
8. J. RODRIGUEZ-CARVAJAL, Full Prof computer program, version 2.1, Har92-ILLJRC (Institut Laue-Langevin, 1992).

Received 31 January 1997

and accepted 7 April 1998